LETTER

doi:10.1038/nature11461

Natural and anthropogenic variations in methane sources during the past two millennia

C. J. Sapart[1], G. Monteil[1], M. Prokopiou[1], R. S. W. van de Wal[1], J. O. Kaplan[2], P. Sperlich[3], K. M. Krumhardt[2], C. van der Veen[1], S. Houweling[1,4], M. C. Krol[1], T. Blunier[3], T. Sowers[5], P. Martinerie[6], E. Witrant[7], D. Dahl-Jensen[3] & T. Röckmann[1]

Methane is an important greenhouse gas that is emitted from multiple natural and anthropogenic sources. Atmospheric methane concentrations have varied on a number of timescales in the past, but what has caused these variations is not always well understood[1–8]. The different sources and sinks of methane have specific isotopic signatures, and the isotopic composition of methane can therefore help to identify the environmental drivers of variations in atmospheric methane concentrations[9]. Here we present high-resolution carbon isotope data ($\delta^{13}C$ content) for methane from two ice cores from Greenland for the past two millennia. We find that the $\delta^{13}C$ content underwent pronounced centennial-scale variations between 100 BC and AD 1600. With the help of two-box model calculations, we show that the centennial-scale variations in isotope ratios can be attributed to changes in pyrogenic and biogenic sources. We find correlations between these source changes and both natural climate variability—such as the Medieval Climate Anomaly and the Little Ice Age—and changes in human population and land use, such as the decline of the Roman empire and the Han dynasty, and the population expansion during the medieval period.

In the pre-industrial period, methane (CH_4) sources can be divided into three categories on the basis of their stable carbon isotopic signatures: biogenic sources (for example, wetlands, rice paddies and ruminants, mean $\delta^{13}C = -60 \pm 5‰$), geological sources[10] (for example, mud volcanoes and microseepages, mean $\delta^{13}C = -38 \pm 7‰$) and pyrogenic sources (for example, fires, biofuel and coal burning, mean $\delta^{13}C = -22 \pm 3‰$)[1–3,9]. The isotopic composition of CH_4 in the troposphere is affected by emissions from these sources and by isotope fractionation in the sink mechanisms, primarily $OH^{\bullet}$ oxidation, with minor contributions from soil removal and stratospheric loss[3].

Previous measurements of the $\delta^{13}C$ value of CH_4 from air trapped in Antarctic ice cores challenged our understanding of the behaviour of pre-industrial CH_4 sources[1,2]. They indicate that before AD 1500, the contribution of ^{13}C-enriched CH_4 sources (for example, biomass burning) had to be larger than expected for pre-industrial conditions in order to explain the generally high $\delta^{13}C$ levels during this period[1–3]. After AD 1500, $\delta^{13}C$ decreased by 2‰ until AD 1800, followed by an abrupt increase presumably caused by increased fossil fuel emissions associated with the onset of industrialization[1–3]. Several hypotheses have been proposed to explain the $\delta^{13}C$ minimum around AD 1800, including a decline in anthropogenic biomass burning in the Americas concurrent with colonial expansion[1], an early rise of ^{13}C-depleted agricultural sources[3] or a combination of both[2].

Our high-resolution $\delta^{13}C$ data from the NEEM (North Greenland Eemian Ice Drilling programme) and EUROCORE ice cores (see Methods) allow a more detailed reconstruction of global-scale changes in CH_4 sources over the past two millennia (Fig. 1a). Whereas the most distinctive feature of the isotopic record over this period is the minimum around AD 1800 (in agreement with previous studies[1,2]), our measurements also reveal three centennial-scale excursions in $\delta^{13}C$ between 100 BC and AD 1600 that were not resolved earlier (Fig. 1a). These excursions are superimposed on a slightly declining long-term trend in $\delta^{13}C$, which is accompanied by a long-term increase in CH_4 mixing ratios of about 70 p.p.b. between 100 BC and AD 1600 as observed in both Northern Hemisphere and Southern Hemisphere records[4–7] (Fig. 1b).

We use a two-box model (see Supplementary Information) to infer possible source/sink variations that are consistent with the observed $\delta^{13}C$ and CH_4 data. In a first step, we vary single sources individually to identify the most important contributors to the isotope variations. The results show that the long-term increase in CH_4 mixing ratios of 70 p.p.b. (corresponding to a source change of 28 Tg CH_4 between 100 BC and AD 1600) cannot originate from geological and pyrogenic sources only, but must be primarily driven by changes in biogenic emissions (Supplementary Fig. 2), in agreement with recent model studies[1,3]. The three centennial-scale $\delta^{13}C$ excursions (Fig. 1a) could be caused by either a relative increase in the ^{13}C-enriched sources (pyrogenic or geological sources) or a decrease in the ^{13}C-depleted

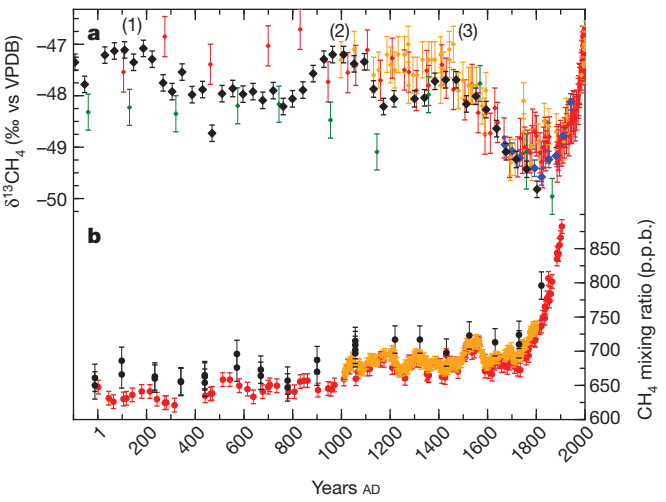

Figure 1 | Records of $\delta^{13}C$ and mixing ratio of CH_4 over the past two millennia. **a**, $\delta^{13}C$ measurements on air trapped in Greenland ice cores from NEEM (black diamonds; this study), EUROCORE (blue diamonds; this study), GISPII[23] (green diamonds) and Antarctic ice cores from Law Dome[1] (red diamonds) and the WAIS divide[2] (orange diamonds). (1), (2) and (3) correspond to the three excursions in the Northern Hemisphere $\delta^{13}C$ record (see main text). **b**, CH_4 mixing ratio records from Greenland (GRIP[5,6]; black circles) and Antarctica (Law Dome[4], red circles; WAIS[7], orange circles). Each data point represents one measurement. Error bars represent $\pm 1\sigma$, based on the reproducibility of the measurement systems.

[1]Institute for Marine and Atmospheric Research Utrecht, Utrecht University, Princetonplein 5, 3584CC Utrecht, The Netherlands. [2]ARVE Group, Ecole Polytechnique Fédérale de Lausanne (EPFL), Station 2, 1015 Lausanne, Switzerland. [3]Center for Ice and Climate, Niels Bohr Institute, University of Copenhagen, Juliane Maries Vej 30, 2100 Copenhagen, Denmark. [4]SRON Netherlands Institute for Space Research, Sorbonnelaan 2, 3584CA Utrecht, The Netherlands. [5]Earth and Environmental Systems Institute, Penn State University, University Park, Pennsylvania 16802, USA. [6]UJF – Grenoble 1/CNRS, Laboratoire de Glaciologie et Géophysique de l'Environnement (LGGE), UMR 5183, F-38041 Grenoble, France. [7]UJF – Grenoble 1/CNRS, Grenoble Image Parole Signal Automatique (GIPSA-lab), UMR 5216, BP 46, F-38402 St Martin d'Hères, France.

©2012 Macmillan Publishers Limited. All rights reserved

sources (biogenic sources). We consider short-term fluctuations in geologic emissions to be unlikely, so our discussion simplifies to biogenic versus pyrogenic sources. The additional constraint that no clear corresponding signal is observed in the CH_4 mixing ratio implies that the isotope variations cannot be explained without variations in pyrogenic sources (Supplementary Fig. 3). Indeed, the larger the difference between the isotopic signature of specific sources and the global mean, the higher its 'isotope leverage', that is, the more effective a change in this source is in changing the overall isotopic composition.

Whereas this single-source approach is suitable for qualitatively identifying the main drivers of the observed variability, it does not help in quantifying simultaneous changes in multiple sources. Thus, in a second step, we mathematically solve the CH_4 and isotope mass balance equations to determine simultaneous variations in the biogenic and the pyrogenic sources that can explain the measured $\delta^{13}C$ and CH_4 mixing ratio data (see Supplementary Information). This multiple-source change approach shows that the centennial-scale $\delta^{13}C$ excursions must be related to increased pyrogenic emissions that are balanced by a concomitant decrease in biogenic emissions.

In order to estimate the uncertainties in the reconstructed source variations, an error propagation study was carried out using a Monte Carlo approach. One thousand simulations were performed, in which model input parameters (observation errors, inter-hemispheric difference in CH_4 and in $\delta^{13}C$, the geological source strength and isotope signatures of the sources) were perturbed randomly within their range of uncertainty (see Supplementary Information). The resulting source reconstructions fall within the light yellow and light green bands in Fig. 2.

In order to further investigate the origin of the reconstructed variations in CH_4 sources, we compared our pyrogenic and biogenic emission scenarios to the Northern Hemisphere charcoal index[11] (based on charcoal accumulation measurements in sediments, and thus a good indicator of biomass burning changes in the past), to model-derived fire activity[12], to the rate of deforestation (estimates based on population data, remote sensed images and land census)[13,14], to precipitation estimates[15], and to reconstructions of Northern Hemisphere[16] and extratropical Northern Hemisphere (NEXT)[17] temperatures (Fig. 2). The Northern Hemisphere charcoal index[11] (Fig. 2c) shows three peaks in biomass burning between 100 BC and AD 1600 that qualitatively coincide in time with the three excursions in $\delta^{13}C$, but the overall correlation is weak. The rate of deforestation is a good indicator of anthropogenic variations in biomass burning because fire was the primary means for land maintenance and clearance (see Supplementary Information). We calculated pyrogenic CH_4 emissions from fires used to clear land and to maintain cropland (see Supplementary Information and Supplementary Fig. 7). The results show that between 100 BC and AD 1600, human activity may have been responsible for roughly 20–30% of the total pyrogenic CH_4 emissions. The anthropogenic fraction increases over time, whereas natural pyrogenic emissions decreased. It is important to note that our estimates of the area under land use[13] include intensification of land use due to new agricultural technologies and population pressure in the last centuries. Therefore the overall land use area increased more slowly than population increase in the recent past. Other estimates of anthropogenic fire activity[12,14] are based on constant per capita land use area. Using these data, CH_4 would scale directly with population, resulting in lower CH_4 emissions from human activity in the past.

The values of $\delta^{13}C$ are high at the beginning of our record and decrease around AD 200 (Fig. 1), which results in a decrease of pyrogenic sources and an increase in biogenic sources in our source reconstruction (Fig. 2a, b). Both the Northern Hemisphere charcoal index (Fig. 2c) and the NEXT temperature reconstruction[17] (Fig. 2f) show decreasing values during this period, for which data on fire activity and precipitation are not available. The decrease in NEXT temperatures could have led to lower CH_4 emissions from wildfires, but a causal link to increasing wetland emissions is less obvious. The data on the rate of

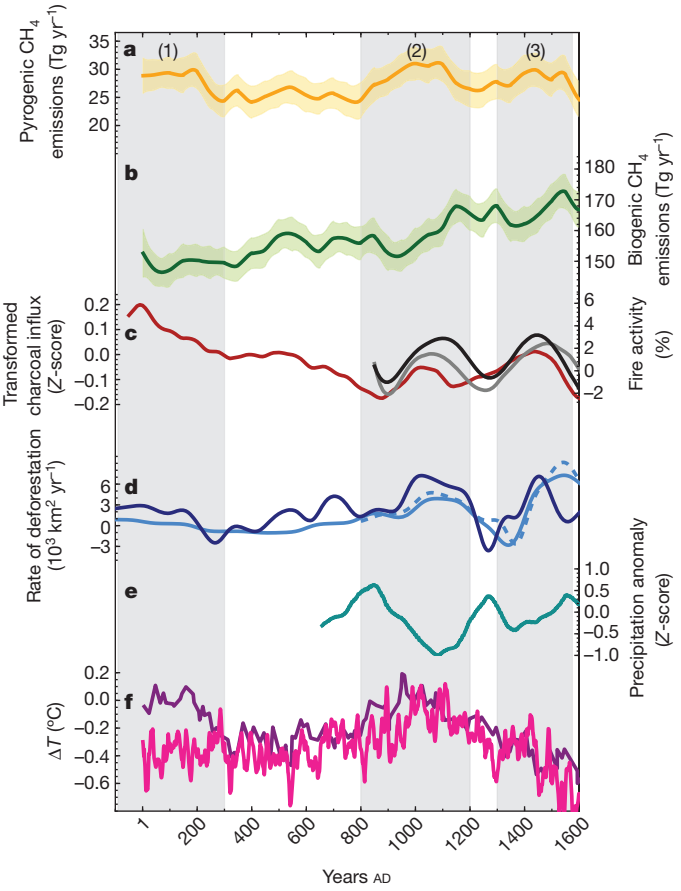

Figure 2 | Reconstructed scenarios for pyrogenic and biogenic CH_4 emissions and other palaeoproxies between 100 BC and AD 1600. Uncertainty envelopes for the source reconstructions are derived from random parameter perturbations in the source inversion (see Supplementary Information). **a**, **b**, Pyrogenic (**a**) and biogenic (**b**) CH_4 emissions. **c**, Northern Hemisphere transformed charcoal index[11] (red curve) and fire activity estimates[12] (model data give percentage of pre-industrial mean) caused by only natural wildfires (grey curve) and by both wildfires and anthropogenic fires (black curve). **d**, Northern Hemisphere rate of deforestation data from KK10[13] (dark blue), HYDE[14] (light blue solid line) and Pongratz[14] (light blue dashed line). **e**, Northern Europe precipitation anomaly[15]. **f**, Northern Hemisphere temperature reconstruction[16] (pink) and Northern Hemisphere extratropics temperature (NEXT) reconstruction[17] (purple). Temperature difference ΔT is with respect to the 1961–90 temperature average. (1), (2) and (3) correspond to the three excursions in the Northern Hemisphere $\delta^{13}C$ record.

anthropogenic deforestation also show a decrease around AD 200, which is related to drastic population declines in China and Europe following the fall of the Han dynasty and the decline of the Roman empire[13]. Rapidly expanding industrial activity between 100 BC and AD 200 in both Europe and East Asia has been reconstructed from heavy-metal pollution detected in a Greenland ice core[18] and sedimentary records[19]. During that time, charcoal was the preferred fuel for industrial and domestic purposes, yielding a large source of ^{13}C-enriched CH_4 (ref. 20). Based on archaeological metal production estimates[21], we calculate that the charcoal used for metal production at the peak of the Roman empire alone could have produced 0.65 Tg yr^{-1} of CH_4. Contemporary civilizations in China and India had similar populations and even more sophisticated metal industries[21]. Although specific estimates of metal production are highly uncertain, we suggest that this early industrial activity may have contributed a sizeable fraction to the ~5 Tg yr^{-1} extra pyrogenic CH_4 emissions before AD 200, according to our model calculation.

The second $\delta^{13}C$ excursion (Fig. 1) correlates very well in timing and duration with the temperature maximum of the Medieval Climate

©2012 Macmillan Publishers Limited. All rights reserved

Anomaly (MCA) that appears in both the Northern Hemisphere and NEXT temperature reconstructions (Fig. 2f) between AD 800 and AD 1200. During this time, our reconstructed scenarios show a temporary decrease in biogenic sources and an increase in pyrogenic sources (Fig. 2). Widespread extended droughts[15] associated with precipitation decrease in Northern Europe (Fig. 2e) provided favourable conditions for enhanced wildfire activity during the MCA. In addition, the medieval period was a time of accelerating deforestation (Fig. 2d) as a result of population expansion and urbanization in Europe and Asia[13], which coincides in time with the second $\delta^{13}C$ excursion observed. Fire activity data (Fig. 2c) provide independent support for both natural and anthropogenic contributions to the increased pyrogenic emissions during this period.

Interestingly, during the MCA the isotopic composition of CH_4 implies generally decreasing biogenic emissions. This seems to contradict the idea that high latitude Northern Hemisphere wetland CH_4 emissions acted as a positive climate feedback to increasing Northern Hemisphere temperatures, which would have led to a decrease in $\delta^{13}C$, contrary to our observations. Increases in methanogenesis rates caused by higher temperatures during this period may have been compensated by decreases in wetland area due to extended droughts[22], leading to a net decrease in biogenic CH_4 emissions.

The third maximum in $\delta^{13}C$ (Fig. 1) occurs simultaneously with the onset of the Little Ice Age (LIA). During this period, Northern Hemisphere temperatures and precipitation decreased (Fig. 2e, f). This may have led to unfavourable conditions for enhanced biogenic emissions. Increased fire activity and charcoal index values during the same period indicate that CH_4 from natural wildfires may have made a significant contribution to the observed $\delta^{13}C$ excursion. In addition, the rate of deforestation (Fig. 2d) shows an increase that is slightly delayed relative to the third $\delta^{13}C$ excursion, suggesting more pyrogenic emissions caused by rapid land clearance during this period.

The long-term trend in mixing ratios and $\delta^{13}C$ values of CH_4 from biogenic sources between 100 BC and AD 1600 (Fig. 1b) can have natural (primarily wetlands[1,6,23]) and anthropogenic (primarily agricultural[2,3,24]) components. Recent model calculations[8] inferred an orbitally-controlled late Holocene increase in global CH_4 levels, primarily driven by increases of Southern Hemisphere tropical natural wetland emissions, which according to this theory are linked to variability in monsoon patterns during the Holocene[25]. On the other hand, we show in Fig. 3 that the long-term trend in CH_4 mixing ratio—that is, the increase between 100 BC and AD 1800—is in very good agreement with reconstructed global anthropogenic land use[13]. This suggests that human activities, including the expansion of rice agriculture[26], played an important role in the observed long-term CH_4 trend over the past two millennia.

Our new isotope data from air trapped in Greenland ice cores allow the reconstruction of variations in different CH_4 source categories over the past 2,100 years. The changes seen in our $\delta^{13}C$ ice core record cannot be explained without variability in biomass burning, which correlates qualitatively with the charcoal index and fire activity data. In addition, we show that the reconstructed source variations are correlated with anthropogenic activities, in particular with long-term increases in agricultural emissions and with varying levels of biomass burning during the period of the Roman empire and the Han dynasty, the MCA and the onset of the LIA. It is thus likely that human activity contributed to variations in CH_4 emissions to the atmosphere long before pre-industrial times.

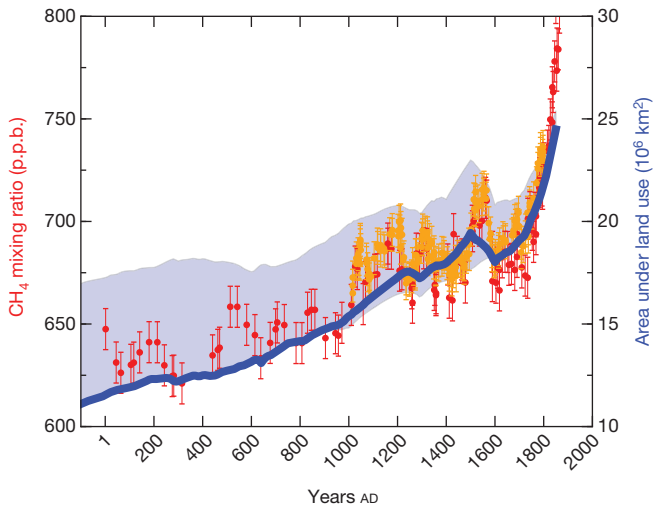

Figure 3 | Comparison between estimate of area under land use and CH_4 mixing ratio. CH_4 mixing ratio records are from the Law Dome[4] (red circles) and WAIS[7] (orange circles) ice cores. The shaded area represents an uncertainty estimate on global area under land use (blue curve, from ref. 13). For details on methods used to construct the land use scenario, see Supplementary Information section 3.

METHODS SUMMARY

We analysed 47 ice samples from the NEEM ice core (North Greenland: site coordinates 77° 27′ N, 51° 4′ W) and 9 from the EUROCORE (Summit, Central Greenland: site coordinates: 72° 34′ N, 38° 27′ W) using a recently developed dry extraction procedure[27] followed by isotope ratio mass spectrometry. A layer of ice (3–5 mm) was microtomed from the surface of the ice to exclude contamination from the drilling liquid and possible anomalies caused by post-coring processes. Samples were not measured in chronological order. Contamination due to sample handling during coring and processing of the ice is very unlikely, because all samples were handled in the same manner and the observed $\delta^{13}C$ variations follow systematic patterns rather than showing an erratic behaviour. No similar temporal patterns are found in the recently obtained dust and ion records of the NEEM core (M. Bigler, personal communication), which makes *in situ* CH_4 formation in the ice also unlikely. Moreover, *in situ* production is very likely to be biogenic and would lead to increases of isotopically depleted CH_4, which are not observed in our profile.

The precision of the $\delta^{13}C$ measurements, based on standards and replicate ice core measurements, is 0.12‰. All $\delta^{13}C$ values are reported versus VPDB (Vienna PeeDee Belemnite). We corrected our data for an inter-laboratory offset of 0.51‰ between our laboratory and Pennsylvania State University[2,23], as determined in a recent intercalibration exercise using real ice core samples[27]. In addition, all isotope data were corrected for gravitational settling, and the four shallowest EUROCORE data were corrected for diffusive fractionation[28]. The age of each ice core air sample was calculated using a delta age (gas age minus ice age) of 183 years for NEEM[29] and 210 years for EUROCORE[30]. Modelled gas age distributions of NEEM and EUROCORE are presented in Supplementary Information.

Received 24 December 2011; accepted 31 July 2012.

1. Ferretti, D. *et al.* Unexpected changes to the global methane budget over the past 2000 years. *Science* **309,** 1714–1717 (2005).
2. Mischler, J. A. *et al.* Carbon and hydrogen isotopic composition of methane over the last 1000 years. *Glob. Biogeochem. Cycles* **23,** GB4024, http://dx.doi.org/10.1029/2009GB003460 (2009).
3. Houweling, S. *et al.* Early anthropogenic CH_4 emissions and the variation of CH_4 and $^{13}CH_4$ over the last millennium. *Glob. Biogeochem. Cycles* **22**(1), http://dx.doi.org/10.1029/2007GB002961 (2008).
4. MacFarling Meure, C. *et al.* Law Dome CO_2, CH_4 and N_2O ice core records extended to 2000 years BP. *Geophys. Res. Lett.* **33,** L14810 http://dx.doi.org/10.1029/2006GL026152 (2006).
5. Blunier, T. *et al.* Variations in atmospheric methane concentration during the Holocene epoch. *Nature* **374,** 46–49 (1995).
6. Chappellaz, J. *et al.* Changes in atmospheric CH_4 gradient between Greenland and Antarctica during Holocene. *J. Geophys. Res.* **102** (D13), 15987–15997 (1997).
7. Mitchell, L. E. *et al.* Multidecadal variability of atmospheric methane, 1000–1800 CE. *J. Geophys. Res.* **116,** G02007, http://dx.doi.org/10.1029/2010JG001441 (2011).
8. Singarayer, J. S. *et al.* Late Holocene methane rise caused by orbitally controlled increase in tropical sources. *Nature* **470,** 82–85 (2011).
9. Quay, P. *et al.* The isotopic composition of atmospheric methane. *Glob. Biogeochem. Cycles* **13,** 445–461 (1999).
10. Etiope, G., Lassey, K. R., Klusman, R. W. & Boschi, E. Reappraisal of the fossil methane budget and related emission from geologic sources. *Geophys. Res. Lett.* **35,** L09307, http://dx.doi.org/10.1029/2008GL033623 (2008).
11. Marlon, J. R. *et al.* Climate and human influences on global biomass burning over the past two millennia. *Nature Geosci.* **1,** 697–702 (2008).
12. Pechony, O. & Shindell, D. T. Driving forces of global wildfires over the past millennium and the forthcoming century. *Proc. Natl Acad. Sci. USA* **107,** 19167–19170 (2010).

©2012 Macmillan Publishers Limited. All rights reserved

13. Kaplan, J. O. *et al.* Holocene carbon emissions as a result of anthropogenic land cover change. *Holocene* **21,** 775–791 (2011).
14. Schmidt, G. A. *et al.* Climate forcing reconstructions for use in PMIP simulations of the last millennium (v1.1). *Geosci. Model Dev.* **5,** 185–191 (2012).
15. Helama, S., Merilainen, J. & Tuomenvirta, H. Multicentennial megadrought in northern Europe coincided with a global El Nino-Southern Oscillation drought pattern during the Medieval Climate Anomaly. *Geology* **37,** 175 (2009).
16. Moberg, A. *et al.* Highly variable Northern Hemisphere temperatures reconstructed from low- and high-resolution proxy data. *Nature* **433,** 613–617 (2005).
17. Ljungqvist, F. C. A new reconstruction of temperature variability in the extra-tropical northern hemisphere during the last two millennia. *Geogr. Annal. A* **92,** 339–351 (2010).
18. Hong, S. M., Candelone, J. P., Patterson, C. C. & Boutron, C. F. History of ancient copper smelting pollution during Roman and medieval times recorded in Greenland ice. *Science* **272,** 246–249 (1996).
19. Brännvall, M. L. *et al.* The Medieval metal industry was the cradle of modern large scale atmospheric lead pollution in northern Europe. *Environ. Sci. Technol.* **33,** 4391–4395 (1999).
20. Akagi, S. K. *et al.* Emission factors for open and domestic biomass burning for use in atmospheric models. *Atmos. Chem. Phys.* **11,** 4039–4072 (2011).
21. Craddock, P. T. *Handbook of Engineering and Technology in the Classical World* Ch. 4 98–120 (Oxford Univ. Press, 2008).
22. Ringeval, B. *et al.* Climate-CH_4 feedback from wetlands and its interaction with the climate-CO_2 feedback. *Biogeosciences* **8,** 2137–2157 (2011).
23. Sowers, T. Atmospheric methane isotope records covering the Holocene period. *Quat. Sci. Rev.* **29,** 213–221 (2010).
24. Ruddiman, W. F. & Thomson, J. S. The case for human causes of increased atmospheric CH_4. *Quat. Sci. Rev.* **20,** 1769–1777 (2001).
25. Burns, S. J. Speleothem records of changes in tropical hydrology over the Holocene and possible implications for atmospheric methane. *Holocene* **21,** 735–741 (2011).
26. Fuller, D. Q. *et al.* The contribution of rice agriculture and livestock pastoralism to prehistoric methane levels: an archaeological assessment. *Holocene* **21,** 743–759 (2011).
27. Sapart, C. J. *et al.* Simultaneous stable isotope analysis of methane and nitrous oxide on ice core samples. *Atmos. Meas. Tech.* **4,** 2607–2618 (2011).
28. Sapart, C. J. *et al.* Reconstruction of the carbon isotopic composition of methane over the last 50 yr based on firn air measurements at 11 polar sites. *Atmos. Chem. Phys. Discuss.* **12,** 9587–9619 (2012).
29. Buizert, C. *et al.* Gas transport in firn: multiple-tracer characterisation and model intercomparison for NEEM, Northern Greenland. *Atmos. Chem. Phys. Discuss.* **11,** 15975–16021 (2011).
30. Schwander, J. *et al.* The age of the air in the firn and the ice at Summit, Greenland. *J. Geophys. Res.* **98** (D2), 2831–2838 (1993).

Supplementary Information is available in the online version of the paper.

Acknowledgements We thank M. Bigler for sharing NEEM CFA dust and ion data; the NEEM community for providing us with ice core samples; and O. Pechony, J. Marlon and Z. Wang for sharing data on fire activity and the charcoal index. This project was supported by the Dutch Science Foundation (NOW; projects 851.30.020 and 865.07.001). NEEM is directed and organized by the Center of Ice and Climate at the Niels Bohr Institute and the US NSF, Office of Polar Programs; it is supported by funding agencies and institutions in Belgium (FNRS-CFB and FWO), Canada (NRCan/GSC), China (CAS), Denmark (FIST), France (IPEV, CNRS/INSU, CEA and ANR), Germany (AWI), Iceland (Rannls), Japan (NIPR), Korea (KOPRI), The Netherlands (NWO/ALW), Sweden (VR), Switzerland (SNF), the UK (NERC) and the USA (US NSF, Office of Polar Programs, ARC 0806407). J.O.K. and K.M.K. were supported by the Swiss National Science Foundation (grant PP0022_119049) and FIRB project CASTANEA (RBID08LNFJ).

Author Contributions C.J.S, T.R, R.S.W.v.d.W., J.O.K. and G.M wrote the manuscript. T.R. and R.S.W.v.d.W. planned and designed the study. C.J.S, T.R., R.S.W.v.d.W., J.O.K., G.M., S.H., M.C.K., K.M.K., P.S., T.S., M.P. and T.B. worked on the scientific interpretation. C.J.S., M.P and C.v.d.V carried out the measurements. G.M., C.J.S., S.H., P.M. and E.W. carried out the modelling work. J.O.K. and K.M.K. provided reconstructions of human land use. D.D.-J. and T.B. led and coordinated the NEEM ice core drilling project and gas consortium.

Author Information Reprints and permissions information is available at www.nature.com/reprints. The authors declare no competing financial interests. Readers are welcome to comment on the online version of the paper. Correspondence and requests for materials should be addressed to C.J.S. (c.j.sapart@uu.nl).

©2012 Macmillan Publishers Limited. All rights reserved